www.amlett.com, www.vbripress.com/aml, DOI: 10.5185/amlett.2014.7593 Published online by the VBRI press in 2014

Preparation and characterization of green gold nanoaprticles conjugate with OMP85 protein

Umesh Kumar Parida[1], S. K. Biswal[2], B.K. Bindhani[1*]

[1]*School of Biotechnology, KIIT University, Bhubaneswar, Odisha, India*
[2]*Department of Chemistry, Centurion University of Technology and Management, Odisha, India*

[*]Corresponding author. Tel: (+91) 674 2725466; E-mail: drbindhani@gmail.com

Received: 11 July 2014, Revised: 23 August 2014 and Accepted: 14 September 2014

ABSTRACT

Gold nanoparticles (AuNPs) have found widespread applications in life sciences. Gold nanoparticles are of interest because of the unique properties which can be incorporated into cancer therapy applications, biosensor materials, composite fibers, cryogenic superconducting materials, cosmetic products, and electronic components. In the present research program, cost effective and environment friendly gold nanoparticles were synthesized using red grape pomace (GPM) ethanolic extract as a reducing agent and a capping agent. The nanoparticles were characterized using UV-visble, XRD, TEM and DLS methods. The absorption peak at 554 nm was found to be broadening with increase in time indicating the polydispersity nature of the nanoparticles. The XRD results suggested that the crystallization of the bioorganic phase occurs on the surface of the gold nanoparticles or vice versa. The TEM image showed relatively spherical shape nanoparticles. We also Purified anti-OMP85 antibody were successfully conjugated on 13 ± 34 nm gold nanoparticles by an electrostatic adsorption method. Copyright © 2014 VBRI press.

Keywords: Green gold; nanomedicine; conjugation; red grape pomace; OMP85 antibody.

Umesh Kumar Parida obtained his M. Sc. in Biotechnology from North Orissa University, Odisha, India. He is presently working as Senior Research Fellow (SRF) of CSIR Project, Govt. of India at School of Biotechnology, KIIT University, Odisha, India. His research interest is "Design and Synthesis of Gold Nanoparticles and Drug Delivery".

Susanta Kumar Biswal is holding the position of Associate Professor in Chemistry at Centurion University of Technology & Management, Odisha, India. He has received his Ph.D. in Chemistry from Utkal Universtiy, Odisha, India. He is now actively engaged in research work in the field of nanotechnology, polymer chemistry, material Science & Environmental Engineering.

B. K. Bindhani is presently working as Assistant Professor-II in the School of Biotechnology, KIIT University, Bhubaneswar, Odisha, India. He has completed his Ph.D. in Botany (Plant Biotechnology) from Utkal University, Bhubaneswar, Odisha, India. Research interests of his laboratory include: *In vitro* culture, Nanobiotechnology, Organic Medical Chemistry, Biochemistry and Environment Science.

Introduction

In the recent years controllable synthesis of noble metal nanoparticles has attracted much attention due to their potential applications in many areas **[1-5]**. Gold nanoparticles have attracted the attention of researchers because of their unique properties, and proven applicability in diverse areas such as medicine, catalysis, textile engineering, biotechnology, nano-biotechnology, bioengineering sciences, electronics **[6-13]**.

Various chemical, physical and biological synthetic methods have been developed to obtain gold nanoparticles of various shapes and sizes, including laser ablation, gamma irradiation, electron irradiation, chemical reduction, photochemical methods, microwave processing, and thermal decomposition of gold oxalate in water and in ethylene glycol, and biological synthetic methods. In biological synthetic methods **[14-17]**, it was shown that the gold nanoparticles produced by plants are more stable in comparison with those produced by other organisms. Plants (especially plant extracts) are able to reduce gold ions faster than fungi or bacteria **[9]**. Furthermore, in order to use easy and safe green methods in scale-up and industrial production of well-dispersed gold nanoparticles, plant extracts are certainly better than plant biomass or living plants **[17]**. However, better experimental procedures are needed for synthesis of well-characterized nanoparticles. It is important to understand the difference between normal

and cancerous tissue to effectively develop hybrid nanoparticles in cancer diagnosis and therapy **[18, 19]**. Normal tissues have tight, continuous vessel walls interspersed with 9 nm pores frequently and 50 nm pores infrequently. Therefore, small molecules can easily penetrate all types of tissues in contrast to large molecules such as polymers that do so very slowly.

AuNPs conjugated to appropriate tumor avid biomolecules with mean sizes in 50-100 nm range are ideal for targeting tumors for imaging and therapy purposes. Connor *et al.* (2005) have shown that gold nanoparticles are inherently non-toxic to human cells despite being taken up into the cells **[20]**. However some precursors used to generate nanoparticles might be toxic **[21]**. This result is significant for the toxicity of gold nanoparticles can be controlled by using non-toxic reagents to produce them. Optical and electronic properties of AuNPs can be utilized to enhance the contrast in molecular imaging for the detection of cancer at early stages. Today, biosynthesis of GNPs using plants or plant extracts, although biosynthesis of gold nanoparticles by plants such as *Perilla frutescens* **[22]**, *Euphorbia hirta* **[23]**, *Punica grantum* **[24]** *Cissus quadrangularis* **[25]** have been reported, the potential of the plants as biological materials for the synthesis of nanoparticles is yet to be fully explored.

In the present research program green synthesis of gold nanoparticles were carried out using the ethanol extract of red grape pomace. Gold nanoparticles through reduction of Au containing salt namely $HAuCl_4$ employing the natural precursor red grape pomace as reductant. Red grape pomace, a wild herbaceous plant is very common in all tropical countries, including India. The Pomace has been widely acknowledged for the treatment of cough, coryza, hay asthma, bronchial infections, bowel complaints, worm infestations, kidney stones in traditional medicine. This prompted the authors of the present paper to investigate the possibility of biosynthesizing GNPs using red grape pomace as biological templates. Novelty of current study, we are first time gold nanoparticles synthesis using ethanol extract of red grape pomace. To the best of our knowledge, these gold nanoparticles will be used for conjugation with protein.

Experimental

Materials

All chemicals were used of analytical grade laboratory reagents. All solutions were prepared with deionised water obtained from a Millipore Milli-Q water system excluding media, which was prepared with distilled water. The chemicals were purchased from Nobel enterprises. Sodium citrate, Hydro Chloroauric acid ($HAuCl_4 \cdot 3H_2O$), b-mercaptoethanol, N-acetyl cysteine (NAc), mercapto succinic acid (MSA), phenylalanine and Tween-20 were purchased from Sigma-Aldrich Ltd., USA. Bio-Rad Bradford assay reagent was used for protein estimation. All reagents were of high quality analytical grade and were filtered immediately before use.

Preparation of pomace extracts

Red wine grape pomace (RGP) (Cabernet Franc) was obtained from a local market (Bhubaneswar, Odisha, India). A portion of the pomace samples (500 g) were immediately freeze-dried upon receiving. The dried extracts were then ground to fine powder by a Thomas Wiley mini-mill (Swedesboro, NJ). The samples were extracted with 80% ethanol at 1:10 ratio (m/v) under overnight shaking. The extracts were filtered through Whatman No.4 filter paper to remove unwanted residues. After evaporating off the organic solvent, the filtrates were frozen and lyophilized to obtain the pomace extracts. A portion of the lyophilized extracts were freshly reconstituted in dimethyl sulfoxide (DMSO) at 20 mg/mL as the stock solution and stored at -20°C for further investigation.

Synthesis of gold nanoparticles

For the synthesis of the gold nanoparticles, a certain volume of the olive RGP (0.1–6 ml) was added to the $HAuCl_4.3H_2O$ solution and the volume was adjusted to 10 ml with de-ionized water. The final concentration of Au was 1.3×10^{-4} M. The reduction process of Au^{3+} to Au nanoparticles was followed by the change in the color of the solution from yellow to violet to dark pink and green depending on the extract concentration **[26, 27]**.

Preparation of antibody–gold nanoparticle conjugates

The 13nm lab made RGP capped gold nanoparticles were used for conjugation. Both the antibody and antigen were affinity purified using protein sepharose and Ni-NTA chromatography respectively. The OMP85 and anti-OMP85 antibody were conjugated to the gold nanoparticles by identical procedures. Critical flocculation concentration (CFC) and the role of different stabilisers were evaluated to optimise the conditions for protein-gold nanoparticle conjugation. To determines the critical flocculation concentration (CFC) of OMP85 antigen and anti-OMP85 antibody for conjugation and stabilization of the gold nanoparticles.

Effect of increasing concentration of stabilizers

Gold nanoparticle-protein conjugates aliquots (100 ml) were dispensed into an ELISA plate as described before. Then, 60 ml of NaCl (to a final optimum concentration) was added to each well. At this stage, all the suspensions were red in colour. This step was followed by the addition of 40 ml of the different stabilisers (Nacetyl cysteine, mercapto succinic acid (MSA), phenylalanine and Tween-20 at varying concentrations. After mixing for 5 minutes, the plates were assessed for aggregation to determine the effect of different stabilisers on the stability of conjugates. The ELISA plates were centrifuged and the supernatants were collected for determination of free protein content using the Bradford assay.

Determination of optimal NaCl concentration (CFC)

These gold nanoparticle conjugates were dispensed in a series (100 ml each) into 96 well ELISA plate. The gold nanoparticle conjugates were then exposed in duplicates to 100 ml of different sodium chloride (NaCl) concentrations (to a final concentration of 0.001 - 2.0 M NaCl in equal volumes). The solutions were agitated for 5 minutes and observed for aggregation to determine the maximum

concentration of NaCl, after which the conjugates were no longer stable. Aggregation was monitored at different wavelengths (490 nm, 595nm, 620 nm and 650 nm) in an ELISA plate reader.

Characterization

The study of UV-vis spectroscopy measurements of the gold nano triangles were carried out using Shimadzu 1600 UV-vis Spectrophotometer (Kyoto, Japan). XRD (X-ray diffraction) analysis was done by using BEDE D-3 system with Cu Kα radiation at a generator or voltage of 40 kV and a generator current of 100 mA. The samples were scanned from scanned from 2θ = 1 – 100° at a scanning rate of 2°/min. A Perkin-Elmer Model of FTIR spectrophotometer, USA within the range of 4000 - 400 cm^{-1} was used for the samples analysis. Approximately, sample of 5 mg was with KBr (100 mg) and condensed into pellet using hydraulic press. The KBr pellet methods were used for all FT-IR spectra analysis. Transmission electron microscopy was performed on a JEOL model 1200EX instrument operated at an accelerating voltage at 80 kV. A Malvern Instrument, MAL 1037088, USA was used to determine the standard size of particle and zeta potential of nanoparticles. Disposable zeta cells measurement was carried with ultra pure water at 25 °C with a −50 mV latex standard calibrated frequently. The mean zeta potential was carried out using phase analysis light scattering technique.

Results and discussion

UV–visible absorption spectrum

Fig. 1 shows the UV–visible absorption spectrum of the RGP and AuNPs in water. The characteristic absorbance peaks at 312 and 554 nm (indicated by an arrow) is clearly observed in RGP-embedded AuNPs in water **[28, 29]**. The symmetric peak indicates that the solution presence of gold nanoparticles. The absorption spectra of this system were periodically rerecorded in the subsequent two months. No obvious change in the shape, position, or symmetry of the absorption peak was observed, which indicates that the as prepared gold nanoparticles can remain stable for at least two months at room temperature.

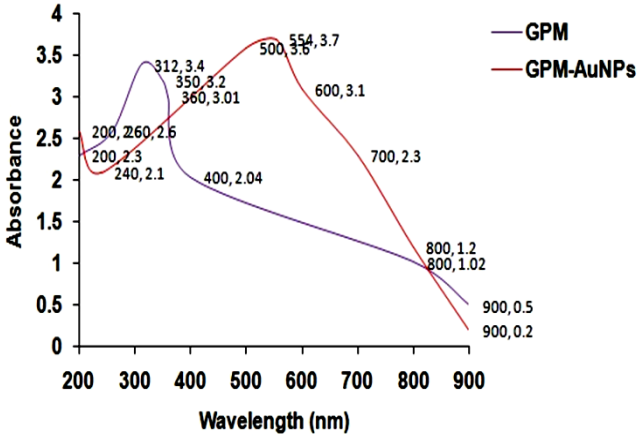

Fig. 1. UV–visible spectrum of RGP extract solution, RGP-AuNPs in water, Arrow indicates the characteristic absorbance peak at 554 nm.

XRD (X-ray diffraction)

In **Fig. 2**, X-ray diffraction patterns of the as-synthesized particles confirmed the formation of gold with crystallite size 13 nm, which is comparable to the particle size calculated from the TEM micrographs (**Fig. 3**). The diffraction peaks for RGP-capped AuNPs was found at 16.7°, 31.2°, 36.4° and 63.2°. The neutral starch effectively coats the positively charged surface of the AuNPs, but the particles retain their positively charged characteristic. This data confirms that the RGP-embedded AuNPs are homogenously coated **[30]**.

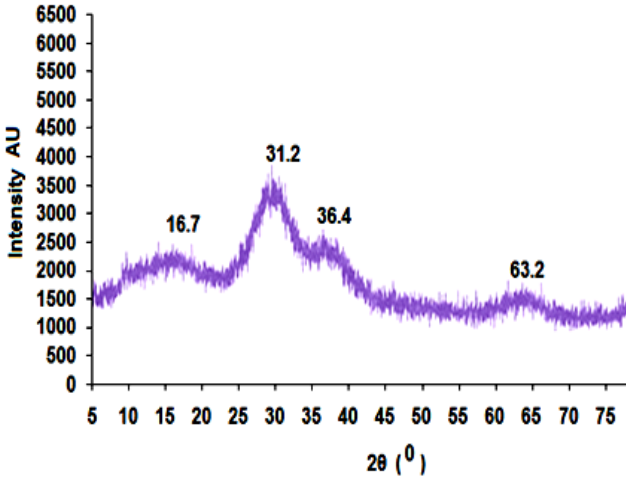

Fig. 2. X-ray diffraction patterns of the as-synthesized metal nanoparticles using RGP extract.

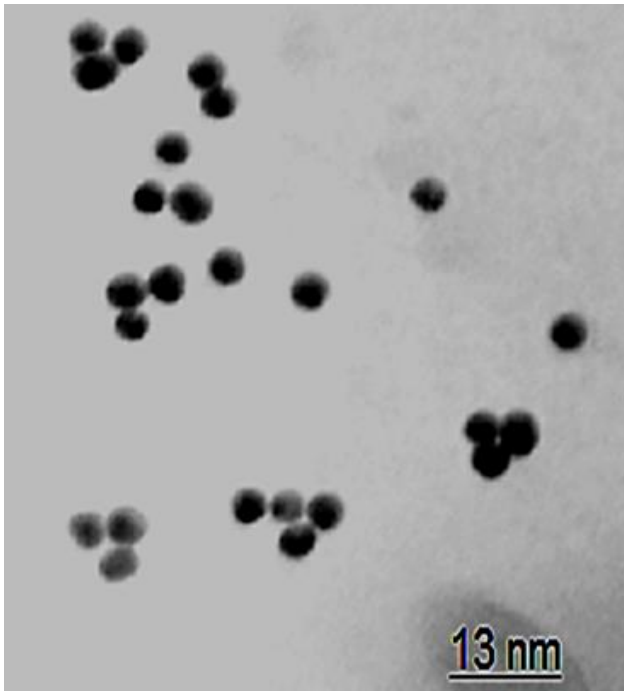

Fig. 3. TEM image of gold nanoparticles.

Transmission electron microscopy (TEM) analysis

Synthesised gold nanoparticles were analysed by transmission electron microscopy. TEM micrographs (**Fig. 3**) showed the presence of spherical gold nanoparticles of approximate size (13 nm) with uniform size distribution

[28]. Although the actual value of the mean size might vary slightly from each preparation, the size distribution was found to be always near about 10% standard deviation. Size distribution analysis clearly showed that nearly 90% of the particles reside within their size range.

Protein-gold nanoparticle conjugation

Critical flocculation concentration: The NaCl solution destabilised the colloid gold nanoparticles and caused aggregation. The sample containing gold nanoparticles and no protein was destabilised immediately upon the addition of electrolytes. As the protein concentration increased, the stability of the nanoparticles also increased which was reflected by a resistance to change from red to blue colour shift. During the flocculation assay, the aggregation was monitored photometrically by the decrease and/or red shift of the plasmon absorption band at different wavelengths of wavelengths of 490nm, 595nm, 620nm and 650nm.

Optimum NaCl concentration

The tube containing the minimum amount of salt to keep the particles stable was indicated by change from red to blue. In the case of both OMP85 antibody conjugation experiments, the particles were stable up to a final concentration of 0.512 M NaCl. Nanoparticles started to aggregate with any concentration of the salt above 0.512 M NaCl (**Fig. 4**).

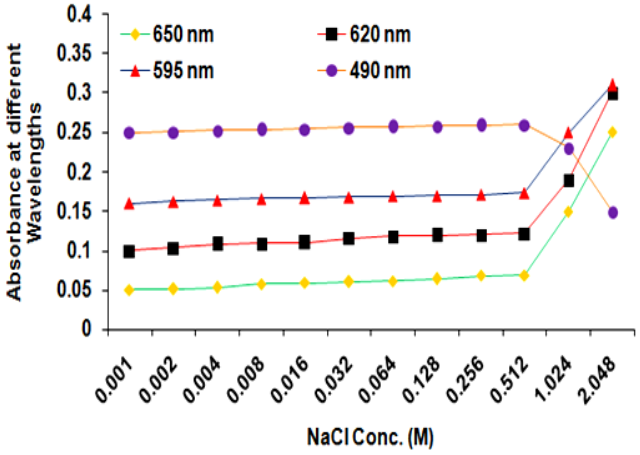

Fig. 4. Critical flocculation concentration of 13 nm gold nanoparticles conjugated with OMP 85 protein were stable up to a final concentration of 0.512 M NaCl.

Effect of stabilizers

The effect of different stabilisers on the increasing or decreasing of stability of gold nanoparticle-protein conjugates did not produce any conclusive results. The presence of NAc and MSA led to aggregation of the conjugates resulting in a colour change from ruby red to blue, despite the fact that analysis of the supernatants using Bradford assay showed that no protein was released or displaced from the aggregated conjugates (**Fig. 5**). Addition of phenylalanine and Tween-20 resulted in no colour change of the conjugates. However, the Bradford assay on the supernatants revealed that and phenylalanine did not displace the bound protein, whereas the particle suspension containing Tween-20 appeared to have protein present in the supernatant suggesting that protein was released from the nanoparticles **[31-33]**.

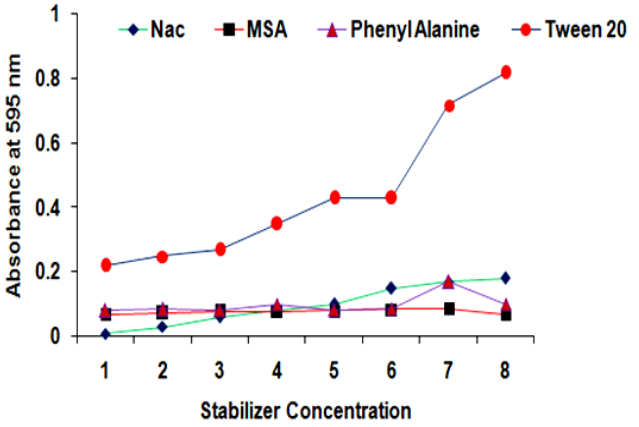

Fig. 5. Effect of increasing concentration of different stabilisers on the 13 nm gold nanoparticle conjugated with OMP85 protein.

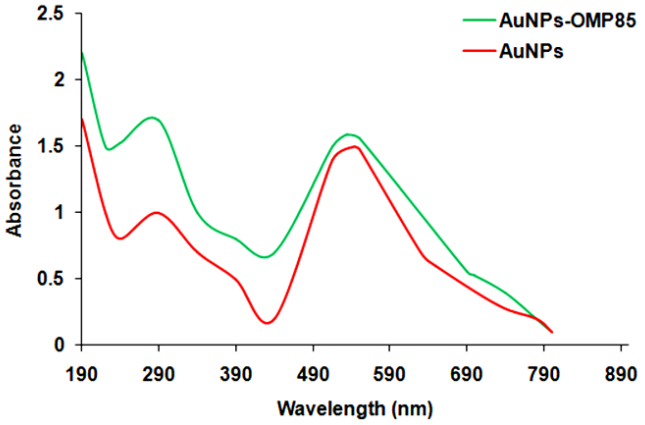

Fig. 6. UV-visible absorbance spectrum of the 13 nm naked nanoparticles and the OMP85 conjugated gold nanoparticles. (a) Increase in absorbance at 280 nm indicating the successful conjugation of nanoparticles and OMP85 protein, (b) 5nm red shift due to the conjugation.

Gold nanoparticle-protein conjugation

Despite some initial inconsistencies with the gold nanoparticles and protein conjugation techniques, conditions were optimised for different sized gold nanoparticles to achieve successful conjugation with OMP 85 antibodies. Unbound proteins and nanoparticles from the nanoparticle-protein conjugates were separated by centrifugation and the conjugated nanoparticles were resuspended in 10 mM sodium phosphate buffer pH 7.4 containing 1% (w/v) BSA and they remained as a ruby red colour during storage. A wavelength scan of the conjugated gold nanoparticles showed slight (~3-5 nm shifts) or no difference from the naked gold nanoparticles (**Fig. 6**). Although conjugated gold nanoparticles are usually more stable, they were stored in a dark vial at 4°C to avoid any instability issues associated with high temperatures.

Conclusion

In conclusion, we have developed an extremely simple route for the synthesis of gold nanoparticles using ethanol pomace extract as a solvent, reducing agent, and capping

agent. Functionalized and biomolecule gold nanoparticles will play an indispensable role in the overall design and development of AuNPs-based nano pharmaceuticals. A completely green route has been developed to synthesize Au nanoparticles in a solution of RGP at a slightly elevated temperature. The route proposed in this work, it seems possible that people can easily make the Au nanoparticles at home. This concept could also be extended to provide strong evidence that AuNPs should be applied to enhance the detection limits in SPR-based bio-specific interaction analysis.

Acknowledgements

Authors are thanks to Director, School of Biotechnology, KIIT University for providing necessary laboratory facilities for this investigation. The Authors also thank to Director CIPET, Chennai and Bhubaneswar for various analytical tests and encouragement.

Reference

1. Li, G.; Tang, Z. *Nanoscale*, **2014**, *6*, 3995. **DOI:** 10.1039/c3nr06787d
2. Su, L.; Jia, W.; Li, C.M.; Lei, Y. *ChemSusChem.*, **2014**, *7*, 361. **DOI:** 10.1002/cssc.201300823
3. Zhang, H.; Jin, M.; Xia, Y. *Angew Chem Int Ed Engl.* **2012**, *51*, 7656. **DOI:** 10.1002/anie.201201557
4. Sailor, M.J.; Park, J.H. *Adv Mater.* **2012**, *24*, 3779. **DOI:** 10.1002/adma.201200653
5. Doria, G.; Conde, J.; Veigas, B.; Giestas, L.; Almeida, C.; Assunção, M.; Rosa, J.; Baptista, P.V. *Sensors (Basel)* **2012**, *12*, 1657. **DOI:** 10.3390/s120201657
6. Parlak, O.; Tiwari, A.; Turner, A.P.F.; Tiwari, A. *Biosens. Bioelectron.* **2013**, *49*, 53.
7. Parlak, O.; Seshadri, P.; Lundström, I.; Turner, APF.; Tiwari, A. *Advanced Materials Interfaces*, **2014**, *1*. **DOI:** 10.1002/admi.201400136
8. Parlak, O.; Turner, A.P.F.; Tiwari, A. *Adv. Mater.* **2014**, *26*, 482.
9. Tiwari, A.; Aryal, S.; Pilla, S.; Gong, S. *Talanta* **2009**, *78*, 1401.
10. Cao, S.; Mishra, R.; Pilla, S.; et al. *Carbohydr. Polym.* **2010**, *82*, 189.
11. Advanced Healthcare Materials, Ashutosh Tiwari (Ed.), Wiley - Scrivener, USA, **2014**; Biosensors Nanotechnology, Ed. Ashutosh Tiwari, Anthony P.F. Turner, Wiley - Scrivener, USA, **2014**; Advanced Energy Materials, Ashutosh Tiwari, Sergiy Valyukh (Eds.), Wiley - Scrivener, USA, **2014**; Advanced Sensor and Detection Materials, Ashutosh Tiwari, Mustafa M. Demir (Eds.), Wiley - Scrivener, USA, **2014**; Advanced Biomaterials and Biodevices, Ashutosh Tiwari, Anis N. Nordin (Eds.), Wiley - Scrivener, USA, **2014**; Advanced Materials for Agriculture, Food and Environmental Safety, Ashutosh Tiwari, Mikael Syväjärvi (Eds.), Wiley - Scrivener, USA, **2014**.
12. Nanomaterials in Drug Delivery, Imaging and Tissue Engineering , Ashutosh Tiwari, Atul Tiwari (Eds.), Wiley - Scrivener , USA, **2013**; Bioengineered Nanomaterials, Ashutosh Tiwari, Atul Tiwari (Eds.), CRC Press, USA, **2013**; Responsive Material Methods and Applications, Ashutosh Tiwari, Hisatoshi Kobayashi (Eds.), Wiley - Scrivener, USA, **2013**; Intelligent Nanomaterials , Ashutosh Tiwari, Ajay K. Mishra, Hisatoshi Kobayashi, Anthony PF Turner (Eds.), Wiley - Scrivener, USA, **2012**; Biomedical Materials and Diagnostic Devices, Ashutosh Tiwari, Murugan Ramalingam, Hisatoshi Kobayashi, Anthony PF Turner (Eds.), Wiley - Scrivener, USA, **2012**; Integrated Biomaterials for Biomedical Technology, Murugan Ramalingam, Ashutosh Tiwari, Seeram Ramakrishna, and Hisatoshi Kobayashi (Eds.), Wiley - Scrivener, USA, **2012**; Smart polymeric materials for biomedical applications, Songjun Li, Ashutosh Tiwari, Mani Prabaharan, Santosh Aryal (Eds.), Nova Science Publishers, Inc., New York, USA, **2010**; Polysaccharides: development, properties and applications ,Ashutosh Tiwari (Ed.), Nova Science Publishers, Inc., New York, USA, **2010**.
13. Recent Developments in Bio- Nanocomposites for Biomedical Applications , Ashutosh Tiwari (Ed.), Nova Science Publishers, Inc., New York, USA, **2010** .
14. Kim, J.H.; Twaddle, K.M.; Hu, J.; Byun, H. *ACS Appl Mater Interfaces*, **2014**, *6*, 11514. **DOI:** 10.1021/am503745w
15. Iyer, R.I.; Panda, T. *J Nanosci Nanotechnol.* **2014**, *14*, 2024. **DOI:** 10.1166/jnn.2014.8897
16. Rai, M.; Yadav, A. *IET Nanobiotechnol*, **2013**, *7*, 117. **DOI:** 10.1049/iet-nbt.2012.0031.
17. Geng, F.; Xing, J.Z.; Chen, J.; Yang, R.; Hao, Y.; Song, K.; Kong, B. *J Biomed Nanotechnol*, **2014**, *10*, 1205. **DOI:** 10.1166/jbn.2014.1855
18. Yang, C.; Neshatian, M.; Van Prooijen, M. *J Nanosci Nanotechnol*, **2014**, *7*, 4813. **DOI:** 10.1166/jnn.2014.9280
19. Connor, E.E.; Mwamuka, J.; Gole, A.; Murphy, C.J.; Wyatt, M.D. *Small*, **2005**, 325. **DOI:** 10.1002/smll.200400093
20. Leung, K. *National Center for Biotechnology Information (US)*, **2008**, 2004 -2013.
21. Basavegowda, N.; Lee, Y.R. *J Nanosci Nanotechnol*, **2014**, *14*, 4377. **DOI:** 10.1166/jnn.2014.8646
22. Annamalai, A.; Christina, V.L.; Sudha, D.; Kalpana, M.; Lakshmi, P.T. *Colloids Surf B Biointerfaces*, **2013**,*108*, 60. **DOI:** 10.1016/j.colsurfb.2013.02.012.
23. Ganeshkumar, M.; Sathishkumar, M.; Ponrasu, T.; Dinesh, M.G.; Suguna, L. *Colloids Surf B Biointerfaces*, **2013**, *106*, 208. **DOI:** 10.1016/j.colsurfb.2013.01.035.
24. Bhuvanasree, S.R.; Harini, D.; Rajaram, A.; Rajaram, R. *Spectrochim Acta A Mol Biomol Spectrosc*, **2013**, *106*, 190. **DOI:** 10.1016/j.saa.2012.12.076.
25. Parida, U.K.; Biswal, S.K.; Bindhani, B.K.; Nayak, P.L. *World Applied Sciences Journal*, **2013**, *28*, 962. **DOI:** 10.5829/idosi.wasj.2013.28.07.13854
26. Parida, U.K.; Bindhani, B.K.; Nayak, P.L. *World Journal of Nano Science and Engineering*, **2011**, *1*, 93. **DOI:** 10.4236/wjnse.2011.14015
27. Fragoon, A.; Li, J.; Zhu, J.; Zhao, J. *J. Nanosci Nanotechnol.* **2012**, *12*, 2337. **DOI:** 10.1166/jnn.2012.5739
28. Tai, Y.; Tran, N. T.; Tsai, Y. C.; Fang, J. Y.; Chang, L. W. *IET Nanobiotechnol.*, **2011**, *5*, 52. **DOI:** 10.1049/iet-nbt.2010.0028.
29. Rajan, A.; Meena Kumari, M.; Philip, D. *Spectrochim Acta A Mol Biomol Spectrosc.*, **2014**, *118*, 793. **DOI:** 10.1016/j.saa.2013.09.086
30. Salehi, M.; Schneider, L.; Ströbel, P.; Marx, A.; Packeisen, J.; Schlücker, S. Nanoscale, **2014**, *6*, 2361. **DOI:** 10.1039/c3nr05890e
31. Humenik, M.; Scheibel, T. *ACS Nano.*, **2014**, *8*, 1342. **DOI:** 10.1021/nn404916f
32. Tatlybaeva, E. B.; Nikiyan, H. N.; Vasilchenko, A. S.; Deryabin, D. G. *Beilstein J Nanotechnol*, **2013**, *4*, 743.
33. Mohamed, M. S.; Veeranarayanan, S.; Poulose, A. C.; Nagaoka, Y.; Minegishi, H.; Yoshida, Y.; Maekawa, T.; Kumar, D. S. *Biochim Biophys Acta.*, **2014**, *1840*, 1657. **DOI:** 10.1016/j.bbagen.2013.12.020